A Sharma–Mittal Geometry of Evenness: Representation, Cardinal Resolution, and Relative Merits

Luca Delvecchio
Universidad de Salamanca, Salamanca, Spain
Email: lucadelvecchio975@gmail.com
September 2026

Abstract

The proliferation of evenness indices creates an interpretive problem whenever several admissible measures assign different numerical values to the same assemblage. We study that problem by normalizing Sharma–Mittal entropy to its maximum at complete uniformity. Written in terms of the Hill number of order α, the resulting surface is

$$\mathcal{E}_{\alpha,\beta}(p;S) = \frac{D_\alpha(p)^{1-\beta} - 1}{S^{1-\beta} - 1}, \qquad \mathcal{E}_{\alpha,1} = \frac{\log D_\alpha}{\log S}.$$

Five canonical Hill-based evenness families are exact restrictions of this surface. More generally, for every $\alpha > 0$ and finite β, the family satisfies Requirements 1a–3b of Chao and Ricotta: transfer, continuity and symmetry, non-increase under addition of a vanishingly rare species, a richness-independent limiting range, and scale invariance. At fixed richness and Hill order, every section is an invertible monotone transformation of the same D_α, so the represented measures contain the same ordinal information and differ in numerical spacing. The parameter β controls that spacing: local sensitivity is proportional to $D_\alpha^{-\beta}$ and the ratio of endpoint slopes is exactly S^β. Over the canonical range $0 \le \beta \le 2$, the largest possible disagreement between any two sections is $(\sqrt{S}-1)/(\sqrt{S}+1)$, attained at $D_\alpha = \sqrt{S}$. When richness differs, ordinal equivalence need not survive: if the linear section and D_α rank two assemblages in opposite directions, continuity guarantees a finite-β ranking reversal. Coverage-standardized Miocene and Pliocene data from Chao et al. (2020) provide a published example, with a crossing near $\beta \approx 1.40$ using their tabulated values. Finally, under K-fold replication, $\beta < 1$ leaves a positive asymptotic evenness deficit, $\beta = 1$ approaches one logarithmically, and $\beta > 1$ approaches one polynomially; at $\beta = 0$ the replication limit is exactly Hill evenness D_α/S. The same parameter also governs independent-product composition and large-richness behavior. These results make the relative merits of alternative evenness geometries explicit without selecting a universal winner.

Keywords: evenness; Sharma–Mittal entropy; Hill numbers; diversity; effective number; generalized entropy; majorization; replication invariance.

1 Introduction

Evenness is intended to describe how equitably total abundance is distributed among the categories of an assemblage. In ecology those categories are species, but the same formal problem arises whenever a finite probability vector describes the allocation of mass, frequency, attention, production, or participation across states. Unlike richness, evenness is not directly counted. It is a normalized judgment about distributional shape, and this has produced a large family of indices based on entropy, concentration, Lorenz ordering, distances from uniformity, effective numbers, and related constructions (Pielou, 1966; Routledge, 1983; Smith and Wilson, 1996; Jost, 2010; Tuomisto, 2012; Kvålseth, 2015).

The measurement problem remains active. Recent work has continued to examine the relation between richness and evenness (Kvålseth, 2024). A sharper critique argues that stand-alone evenness can be unstable or weakly connected to ecological process (Alroy, 2025; Warren, 2026), while recent counterevidence emphasizes that relative-abundance evenness can have direct and mediating associations with ecosystem services (Hordijk, 2026). The present paper addresses a narrower question on which these positions need not disagree. It does not attempt to establish evenness as a causal ecological state variable. Conditional on using evenness as a descriptive measure, it asks what exactly changes when one admissible numerical representation is chosen instead of another.

The difficulty is not merely that many indices exist. Several measures satisfy closely related basic requirements while assigning substantially different values to the same assemblage. Chao and Ricotta (2019), building on Hill-number diversity, systematized five classes satisfying the transfer principle, continuity and symmetry, a richness-related condition for addition of a vanishingly rare species, a fixed limiting range, and scale invariance. Their framework clarifies the relation between diversity and evenness, but an interpretive question remains: if several classes are admissible, what property of measurement changes with the choice among them?

A recent perspective sharpens the issue from a different direction. Chisholm (2026) advocates Lorenz-consistent evenness, including replication invariance, and contrasts that program with value-constrained normalizations whose minimum and maximum do not depend on richness. If replication invariance is dropped and the value-constraint requirement is admitted, Pielou's index and Heip's index become canonical examples of the alternative axiomatization. Chao and Ricotta's five classes belong to the same value-constrained tradition and satisfy replication monotonicity rather than replication invariance. This conflict is not removed by introducing another formula; it can, however, be made quantitative.

Parametric evenness itself is not new. Hill (1973) proposed a double continuum based on ratios of effective diversities; Ricotta and Avena (2002) gave an information-theoretical interpretation of Hill's parametric evenness; and Ricotta (2003) reviewed broader parametric evenness families and their relation to Lorenz ordering, richness, and diversity. Those constructions vary one or two diversity orders. The construction studied here is different. At a fixed Hill order α, the underlying effective diversity is held fixed while a second parameter changes only its normalized numerical representation relative to richness.

The Sharma–Mittal family provides a natural coordinate system for isolating that operation. Sharma–Mittal entropy is a two-parameter generalized entropy containing Rényi and Tsallis forms as limiting or restricted cases (Sharma and Mittal, 1975; Rényi, 1961; Tsallis, 1988). Its application to diversity is also established. Hoffmann (2008) developed a broad Sharma–Mittal unification of distribution-based diversity measures, and Crupi (2019) explicitly represented biological diversity measures in a Sharma–Mittal order–degree plane, emphasizing that the order parameter controls sensitivity to rare categories while the degree parameter changes metric properties. Introducing Sharma–Mittal entropy to biodiversity is therefore not the contribution of this paper.

Maximum normalization is used here as a construction step, not claimed as a novelty in itself. Rewriting Sharma–Mittal entropy through Hill numbers and dividing by its value at complete uniformity produces a two-parameter evenness surface. On that surface, α determines which distributional information is summarized, by setting the Hill order and therefore the relative emphasis on rare and dominant categories, while β determines how that order-specific effective diversity is numerically spaced between maximal concentration and complete uniformity. Throughout, *cardinal* is used in this operational sense of numerical spacing on the normalized scale. It is not a claim that ecological evenness has a uniquely privileged interval or ratio scale.

This separation motivates three questions. First, do the principal Hill-based evenness classes contain different scalar distributional information at a common order, or are they alternative numerical representations of the same information? Second, what does β change in local and global numerical resolution, especially when richness differs or assemblages are replicated? Third, which substantive criteria can justify choosing one geometry rather than another?

The aim is not to add another index. Fixed-order equivalence among generalized entropy representations is established territory: number-equivalent arguments already show that monotone generalized entropies of a common order encode the same effective diversity (Jost, 2009). We use that fact as a starting point. The results specific to the present construction are that the entire finite-β normalized surface satisfies the Chao–Ricotta requirements; their five Hill-based classes are exact paths on it; and the resulting geometry yields explicit local and global bounds on numerical resolution, a sufficient criterion for cross-richness ranking reversals, a replication-response trichotomy, normalized product-composition laws, and richness-scaling consequences. The framework therefore turns the selection of an evenness formula from a catalog choice into an explicit choice among numerical standards.

2 The normalized Sharma–Mittal evenness surface

2.1 Hill numbers and effective diversity

Let $p = (p_1, \ldots, p_S)$ be a probability vector on its positive support, with $S \geq 2$, $p_i > 0$, and $\sum_i p_i = 1$. Thus S is realized richness. Maximal concentration is understood as the boundary limit $p_1 \to 1$ and $p_i \to 0^+$ for $i > 1$. If an externally fixed universe retains zero-mass categories, the same formulas remain valid with S interpreted as category capacity rather than realized richness.

For $\alpha > 0$, $\alpha \neq 1$, the Hill number of order α is (Hill, 1973)

$$D_\alpha(p) = \left(\sum_{i=1}^{S} p_i^\alpha \right)^{1/(1-\alpha)}. \tag{1}$$

At $\alpha = 1$, continuity gives

$$D_1(p) = \exp\left(-\sum_{i=1}^{S} p_i \log p_i \right). \tag{2}$$

Hence $1 \leq D_\alpha \leq S$. Complete uniformity gives $D_\alpha = S$, while maximal concentration gives $D_\alpha \to 1$. For a non-uniform distribution, D_α is non-increasing in α: lower orders give relatively greater weight to rare categories and higher orders to dominant categories (Hill, 1973; Chao et al., 2014).

2.2 Sharma–Mittal entropy and normalization

For $\alpha \neq 1$ and $\beta \neq 1$, Sharma–Mittal entropy can be written as

$$\mathrm{SM}_{\alpha,\beta}(p) = \frac{\left(\sum_i p_i^\alpha\right)^{(1-\beta)/(1-\alpha)} - 1}{1-\beta}. \tag{3}$$

Using Eq. (1),

$$\mathrm{SM}_{\alpha,\beta}(p) = \frac{D_\alpha(p)^{1-\beta} - 1}{1-\beta}. \tag{4}$$

At complete uniformity,

$$\mathrm{SM}^{\max}_{\alpha,\beta}(S) = \frac{S^{1-\beta} - 1}{1-\beta}. \tag{5}$$

Definition 1 (Normalized Sharma–Mittal evenness)**.** *For $\alpha > 0$ and $\beta \neq 1$, define*

$$\mathcal{E}_{\alpha,\beta}(p; S) = \frac{D_\alpha(p)^{1-\beta} - 1}{S^{1-\beta} - 1}, \tag{6}$$

and at $\beta = 1$ define the continuous section

$$\mathcal{E}_{\alpha,1}(p; S) = \frac{\log D_\alpha(p)}{\log S}. \tag{7}$$

For $\alpha = 1$, Eq. (6) is understood through the continuous Hill number D_1 above. Equivalently,

$$\mathcal{E}_{\alpha,\beta} = \frac{\ln_\beta D_\alpha}{\ln_\beta S}, \qquad \ln_\beta x = \frac{x^{1-\beta} - 1}{1 - \beta},$$

with the ordinary logarithm recovered at $\beta = 1$.

Proposition 2 (Range and endpoints)**.** *For $S \geq 2$, $\alpha > 0$, and finite β, $0 \leq \mathcal{E}_{\alpha,\beta} \leq 1$. The maximum 1 is attained only at uniformity. On the positive-support domain the minimum is approached as $D_\alpha \to 1$; the closure of the attainable range is therefore $[0, 1]$.*

Proof. For fixed β, $x \mapsto (x^{1-\beta} - 1)/(1 - \beta)$ is strictly increasing for $x > 0$. Since $1 \leq D_\alpha \leq S$, normalization by its value at S gives the result. The logarithmic case follows by continuity. □

Proposition 3 (Admissibility under the Chao–Ricotta requirements)**.** *For every $S \geq 2$, $\alpha > 0$, and finite β, $\mathcal{E}_{\alpha,\beta}$ satisfies Requirements 1a, 1b, 2, 3a, and 3b of Chao and Ricotta (2019): transfer, continuity and symmetry, non-increase when a vanishingly rare category is added while order-α diversity changes negligibly, a fixed limiting range, and scale invariance.*

Proof. At fixed S and β, $\mathcal{E}_{\alpha,\beta}$ is strictly increasing in D_α. For $\beta \neq 1$,

$$\frac{\partial \mathcal{E}_{\alpha,\beta}}{\partial D_\alpha} = \frac{(1 - \beta) D_\alpha^{-\beta}}{S^{1-\beta} - 1} > 0, \tag{8}$$

and at $\beta = 1$ the derivative is $(D_\alpha \log S)^{-1} > 0$. Hill diversity is strictly Schur-concave for $\alpha > 0$ in the standard majorization sense (Marshall et al., 2011), so the transfer principle is inherited; continuity and permutation symmetry are inherited as well. The preceding proposition gives the richness-independent limiting range, and multiplying all raw abundances by a common positive constant leaves p, D_α, and $\mathcal{E}_{\alpha,\beta}$ unchanged.

For Requirement 2, hold $D_\alpha > 1$ fixed and treat richness as a continuous argument. For $\beta \neq 1$,

$$\frac{\partial \mathcal{E}_{\alpha,\beta}}{\partial S} = -\frac{(1 - \beta) S^{-\beta} (D_\alpha^{1-\beta} - 1)}{(S^{1-\beta} - 1)^2} < 0, \tag{9}$$

and for $\beta = 1$,

$$\frac{\partial \mathcal{E}_{\alpha,1}}{\partial S} = -\frac{\log D_\alpha}{S (\log S)^2} < 0.$$

Adding a category of abundance $\varepsilon \to 0^+$ increases support size by one while D_α converges to its pre-addition value for every $\alpha > 0$. Continuity therefore gives the required non-increase in the vanishing-abundance limit. If $D_\alpha = 1$, the measure remains at its lower boundary value. □

Two reductions orient the surface. The limit $\beta \to 1$ yields Rényi entropy before normalization; the line $\beta = \alpha$ yields the Tsallis branch; and the joint limit $(\alpha, \beta) \to (1, 1)$ gives Shannon entropy (Shannon, 1948). Holding $\beta \neq 1$ fixed while taking $\alpha \to 1$ instead yields a β-deformed function of Shannon entropy, not Shannon entropy itself.

3 Representation and ordinal structure

3.1 Five canonical Hill-based families

Theorem 4 (Representation theorem)**.** *Let $D_\alpha = D_\alpha(p)$. The five Hill-number-based evenness families tabulated by Chao and Ricotta (2019) are restrictions of the normalized Sharma–Mittal surface:*

$$E_1^\alpha(p) = \mathcal{E}_{\alpha,\alpha}(p; S) = \frac{D_\alpha^{1-\alpha} - 1}{S^{1-\alpha} - 1}, \tag{10}$$

$$E_2^\alpha(p) = \mathcal{E}_{\alpha,2-\alpha}(p; S) = \frac{D_\alpha^{\alpha-1} - 1}{S^{\alpha-1} - 1}, \tag{11}$$

$$E_3^\alpha(p) = \mathcal{E}_{\alpha,0}(p; S) = \frac{D_\alpha - 1}{S - 1}, \tag{12}$$

$$E_4^\alpha(p) = \mathcal{E}_{\alpha,2}(p; S) = \frac{1 - D_\alpha^{-1}}{1 - S^{-1}}, \tag{13}$$

$$E_5^\alpha(p) = \mathcal{E}_{\alpha,1}(p; S) = \frac{\log D_\alpha}{\log S}. \tag{14}$$

Proof. Substitute $\beta = \alpha$, $\beta = 2 - \alpha$, $\beta = 0$, $\beta = 2$, and the continuous limit $\beta = 1$ into Eqs. (6)–(7). For the first two paths, $D_\alpha^{1-\alpha} = \sum_i p_i^\alpha$ and $D_\alpha^{\alpha-1} = (\sum_i p_i^\alpha)^{-1}$. □

The theorem concerns the five Hill-based classes. The Minkowski-distance family included as a separate comparison row by Chao and Ricotta (2019) is not part of the representation; Section 8.7 returns to this boundary case.

The five paths have two geometrically different forms. E_3, E_5, and E_4 keep β fixed at 0, 1, and 2, so α alone changes the distributional order. E_1 and E_2 couple the cardinal parameter to the diversity order along the diagonal and anti-diagonal. Figure 1 displays the canonical region $0 < \alpha \leq 2$, $0 \leq \beta \leq 2$. The boundary $\alpha = 0$ is degenerate here because $D_0 = S$ and hence $\mathcal{E}_{0,\beta} = 1$ for every β.

Following the attributions in Chao and Ricotta (2019), $(\alpha, \beta) = (1, 1)$ gives Pielou's Shannon evenness (Pielou, 1966), $(1, 0)$ gives Heip's form (Heip, 1974), and $(2, 0)$ gives the Kvålseth special case (Kvålseth, 1991) shared by E_2 and E_3. At $\alpha = 2$, the E_5 point and the coincident E_1/E_4 point are Smith–Wilson special cases (Smith and Wilson, 1996). The general E_1 path is attributed by Chao and Ricotta to Mendes et al. (2008).

3.2 Ordinal equivalence

Theorem 5 (Ordinal equivalence at fixed richness and order)**.** *Fix S and α. For any finite β_1, β_2 and any two distributions p, q on S categories,*

$$\mathcal{E}_{\alpha,\beta_1}(p; S) > \mathcal{E}_{\alpha,\beta_1}(q; S) \iff \mathcal{E}_{\alpha,\beta_2}(p; S) > \mathcal{E}_{\alpha,\beta_2}(q; S).$$

Equality is likewise preserved.

Proof. For fixed S and β, Eqs. (6)–(7) are strictly increasing functions of D_α. □

Corollary 6 (No additional scalar distributional information)**.** *At fixed S and α, any one value $\mathcal{E}_{\alpha,\beta}$ determines D_α exactly and therefore determines every other $\mathcal{E}_{\alpha,\beta'}$. The represented classes differ in numerical geometry, not in ordinal information.*

The common dependence on D_α is already visible algebraically in Chao and Ricotta's formulas, and the broader numbers-equivalent argument for fixed-order generalized entropies is not new (Jost, 2009). Here ordinal equivalence is used as a structural lemma: once order-specific effective diversity

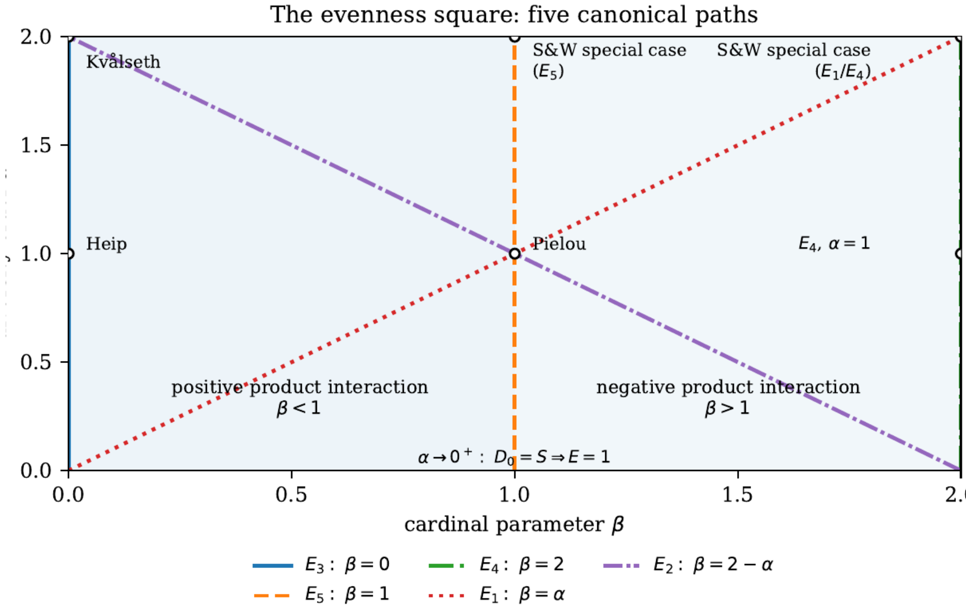

Figure 1: The evenness square. Five canonical restrictions of the normalized Sharma–Mittal plane over $0 \le \beta \le 2$ and $0 < \alpha \le 2$. The background labels the sign of the interaction term under independent-product composition of the unnormalized generator; this is distinct from subadditivity on the majorization lattice.

is fixed, a scientifically relevant difference among the represented classes must concern the numerical map applied to it. This conclusion is deliberately narrow: measures outside the Hill-sufficient class may retain information not compressed into a single D_α, and comparisons that change S or α are not covered by the fixed-S, fixed-α equivalence.

3.3 Cross-richness rank reversals

Theorem 5 is a fixed-richness statement. When richness changes, the denominator that normalizes D_α changes as well, and a common ranking is no longer guaranteed. The limiting geometry makes one sufficient condition explicit.

For a non-degenerate assemblage with $1 < D_\alpha < S$, as $\beta \to \infty$,

$$1 - \mathcal{E}_{\alpha,\beta} = \frac{D_\alpha^{1-\beta} - S^{1-\beta}}{1 - S^{1-\beta}} \sim D_\alpha^{1-\beta}. \tag{15}$$

Thus, for sufficiently large β, the ranking is determined by D_α alone, even though the numerical values themselves approach one.

Proposition 7 (A sufficient rank-reversal criterion)**.** *Consider two assemblages A and B at a common Hill order α, with $1 < D_A < S_A$ and $1 < D_B < S_B$. If*

$$\left[\frac{D_A - 1}{S_A - 1} - \frac{D_B - 1}{S_B - 1}\right](D_A - D_B) < 0, \tag{16}$$

then there exists at least one finite $\beta^* > 0$ such that

$$\mathcal{E}_{\alpha,\beta^*}(A) = \mathcal{E}_{\alpha,\beta^*}(B).$$

Proof. At $\beta = 0$, the two assemblages are ordered by $(D - 1)/(S - 1)$. By Eq. (15), for sufficiently large β they are ordered by D itself. Condition (16) states that these two orderings have opposite signs. Continuity of $\mathcal{E}_{\alpha,\beta}$ in β therefore gives at least one crossing. □

The condition is sufficient, not claimed to be necessary, and no uniqueness claim is required here. Its role is narrower: it identifies a transparent circumstance in which changing cardinal geometry can reverse a cross-richness comparison even though the Hill order is held fixed.

Proposition 8 (Reversal inside the canonical square)**.** *Consider two assemblages A and B at a common Hill order α, with $1 < D_A < S_A$ and $1 < D_B < S_B$. If*

$$[\mathcal{E}_{\alpha,0}(A) - \mathcal{E}_{\alpha,0}(B)]\,[\mathcal{E}_{\alpha,2}(A) - \mathcal{E}_{\alpha,2}(B)] < 0,$$

then at least one crossing occurs at some $\beta^* \in (0, 2)$. Equivalently, the hypothesis says that the canonical classes E_3 and E_4 rank the two assemblages in opposite directions.

Proof. The map $\beta \mapsto \mathcal{E}_{\alpha,\beta}$ is continuous, so opposite orderings at the two endpoints $\beta = 0$ and $\beta = 2$ imply a crossing in the open interval. □

This proposition is deliberately local to the canonical square. Proposition 7 guarantees a finite crossing under its sufficient condition but does not locate that crossing relative to $\beta = 2$; Proposition 8 shows directly when the disagreement is already visible between the linear and reciprocal classes used throughout the paper. When the reciprocal section has nearly saturated, such reversals may remain ordinally real but cardinally small, linking the rank question to the resolution result of Section 4.2.

4 Cardinal geometry: what does β mean?

4.1 Equal numerical values do not represent equal effective diversity

For $\beta \neq 1$, Eq. (6) can be inverted:

$$D_\alpha = \left[1 + E\left(S^{1-\beta} - 1\right)\right]^{1/(1-\beta)}, \tag{17}$$

where $E = \mathcal{E}_{\alpha,\beta}$. At $\beta = 1$,

$$D_\alpha = S^E. \tag{18}$$

Thus identical values on $[0, 1]$ can correspond to very different effective diversities. With $S = 100$ and $E = 0.5$,

$$\beta = 0: \; D_\alpha = 50.5, \qquad \beta = 1: \; D_\alpha = 10, \qquad \beta = 2: \; D_\alpha = \frac{200}{101} \approx 1.98.$$

The same range therefore does not imply the same numerical semantics across different cardinal maps.

4.2 Local resolution

Proposition 9 (Local resolution)**.** *For $\beta \neq 1$,*

$$\frac{\partial \mathcal{E}_{\alpha,\beta}}{\partial D_\alpha} = \frac{(1-\beta) D_\alpha^{-\beta}}{S^{1-\beta} - 1} > 0,$$

and at $\beta = 1$,

$$\frac{\partial \mathcal{E}_{\alpha,1}}{\partial D_\alpha} = \frac{1}{D_\alpha \log S}.$$

For $\beta > 0$ the map is strictly concave in D_α; it is linear at $\beta = 0$ and convex if extended to $\beta < 0$.

Within the canonical range $0 \leq \beta \leq 2$, increasing β progressively shifts local numerical resolution toward the concentrated end $D_\alpha \approx 1$.

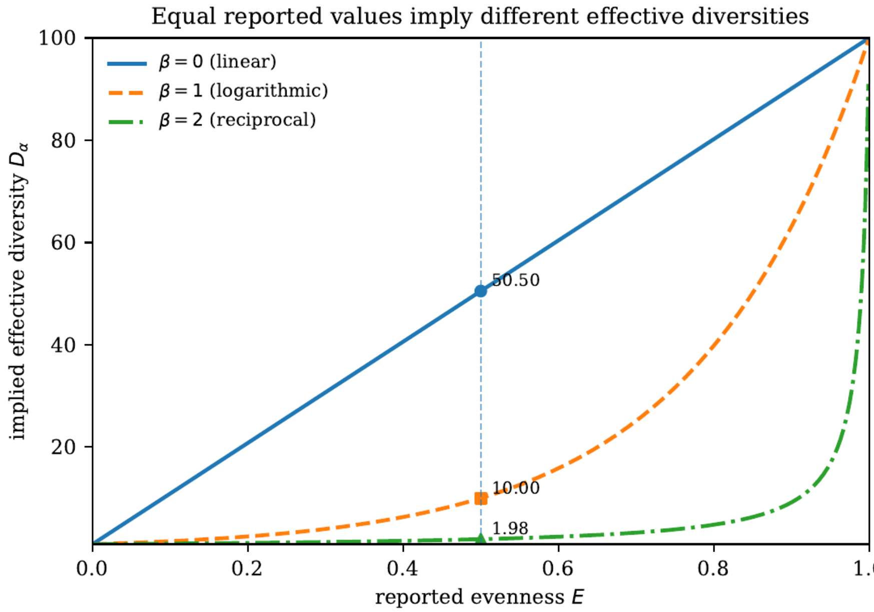

Figure 2: Equal reported values across classes need not represent equal effective diversity. For $S = 100$, the value $E = 0.5$ corresponds to $D_\alpha = 50.5$, 10, and approximately 1.98 under the linear, logarithmic, and reciprocal geometries.

Corollary 10 (Resolution-skew ratio)**.** *Define the ratio of endpoint slopes*

$$\mathcal{R}_\beta(S) = \frac{\partial E/\partial D_\alpha|_{D_\alpha=1}}{\partial E/\partial D_\alpha|_{D_\alpha=S}}.$$

Then

$$\mathcal{R}_\beta(S) = S^\beta. \tag{19}$$

Thus $\beta = 0$ gives equal absolute resolution throughout the effective-diversity interval, $\beta = 1$ gives S times more local resolution near maximal concentration than near uniformity, and $\beta = 2$ gives S^2 times more.

4.3 Monotonic ordering and maximum cardinal spread

Theorem 11 (Monotonicity in the cardinal parameter)**.** *Fix $S > 1$, $\alpha > 0$, and a non-uniform distribution with $1 < D_\alpha < S$. Then $\mathcal{E}_{\alpha,\beta}$ is strictly increasing in β. In particular,*

$$E_4^\alpha > E_5^\alpha > E_3^\alpha.$$

A proof is given in Appendix A. The result orders the fixed geometries numerically without changing their common assemblage ordering at fixed richness.

Monotonicity also allows a global question that local slope ratios do not answer: how far apart can two cardinalizations be on the canonical square?

Theorem 12 (Maximum cardinal spread on $0 \le \beta \le 2$)**.** *Fix $S > 1$ and $\alpha > 0$. Across all effective diversities $D_\alpha \in [1, S]$ and all $\beta_1, \beta_2 \in [0, 2]$,*

$$\sup_{D_\alpha} \sup_{\beta_1,\beta_2 \in [0,2]} |\mathcal{E}_{\alpha,\beta_2} - \mathcal{E}_{\alpha,\beta_1}| = \frac{\sqrt{S} - 1}{\sqrt{S} + 1}. \tag{20}$$

The maximum is attained by the extreme sections $\beta = 0$ and $\beta = 2$ at $D_\alpha = \sqrt{S}$, equivalently at $\mathcal{E}_{\alpha,1} = 1/2$.

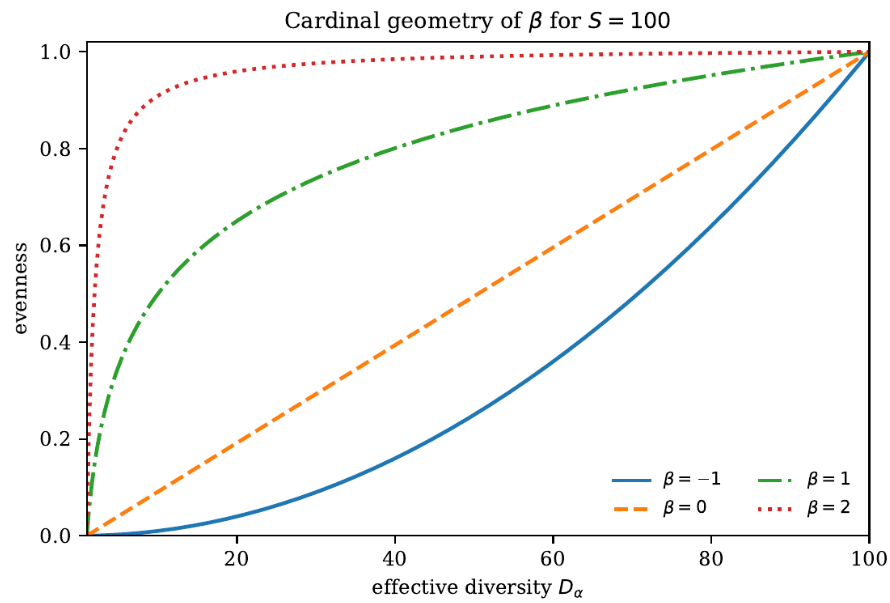

Figure 3: Cardinal geometry of β for $S = 100$. Positive β increases concavity and reallocates numerical resolution toward low effective diversity. The $\beta = -1$ curve is shown only as a mathematical continuation outside the canonical square.

Proof. By monotonicity in β, the largest difference at fixed D_α is $\mathcal{E}_{\alpha,2} - \mathcal{E}_{\alpha,0}$. Direct calculation gives

$$\mathcal{E}_{\alpha,2} - \mathcal{E}_{\alpha,0} = \frac{(D_\alpha - 1)(S - D_\alpha)}{D_\alpha(S - 1)}.$$

Writing this as $[S + 1 - D_\alpha - S/D_\alpha]/(S - 1)$, differentiation gives a unique maximum at $D_\alpha = \sqrt{S}$; the second derivative is negative. Substitution yields Eq. (20). Finally, $\log(\sqrt{S})/\log S = 1/2$. The maximizing value is attainable along any continuous path in the simplex whose Hill diversity ranges from S toward 1. $\square$

The bound complements the local skew S^β. The skew can be very large even when the total possible displacement on the normalized scale is more modest. The global bound equals $3 - 2\sqrt{2} \approx 0.1716$ for $S = 2$, $1/3$ for $S = 4$, $1/2$ for $S = 9$, and approaches one only as richness becomes large. Thus the cardinal freedom available to β is itself richness-dependent in an exactly quantifiable way.

5 Criteria for choosing β

The observed probability vector does not identify a preferred β. A choice must therefore appeal to a criterion external to the distribution. The first three criteria below concern the numerical purpose of the measure. Replication is different: replication invariance lies outside the present value-constrained family and therefore supplies a benchmark against which the sections can be compared.

5.1 Discriminative target

If equal absolute increments in effective diversity should receive equal numerical weight, $\beta = 0$ is the unique linear section. If the application is mainly concerned with distinguishing extreme concentration from modest diversification, positive β shifts resolution toward low D_α, increasingly so as β rises. An extension to $\beta < 0$ reverses the allocation and emphasizes differences among already even assemblages, although that region lies outside the canonical square.

This criterion has a substantive interpretation. An early-warning indicator for monopolization, ecological dominance, or portfolio concentration may reasonably devote most of its resolution to the neighborhood of $D_\alpha = 1$. By contrast, an index intended to express affine occupation of the available effective-diversity interval has a natural reason to retain $\beta = 0$. The global bound in Eq. (20) additionally states how much these choices can matter in total at a given richness.

5.2 Independent-product composition and lattice properties

For independent systems, Hill numbers multiply:

$$D_\alpha(A \times B) = D_\alpha(A) D_\alpha(B). \tag{21}$$

Substitution into unnormalized Sharma–Mittal entropy gives the pseudo-additive identity

$$\mathrm{SM}_{\alpha,\beta}(A \times B) = \mathrm{SM}_{\alpha,\beta}(A) + \mathrm{SM}_{\alpha,\beta}(B) + (1-\beta)\mathrm{SM}_{\alpha,\beta}(A)\mathrm{SM}_{\alpha,\beta}(B). \tag{22}$$

The interaction relative to ordinary additivity is positive for $\beta < 1$, zero at $\beta = 1$, and negative for $\beta > 1$.

This product identity must not be conflated with subadditivity or supermodularity on the majorization lattice. Bruno and Vaccaro's current preprint proves, among other results, lattice subadditivity for $\alpha \geq 0$, $\beta \geq 1$, and supermodularity for $\alpha > 0$, $\beta \leq \alpha$ (Bruno and Vaccaro, 2026). On the interior of a fixed-S simplex, meet and join preserve full support, so the common maximum-normalization factor is the same for all four lattice terms; the corresponding inequalities therefore transfer to normalized evenness. Details and the placement of the five canonical paths are recorded in Appendix B. These lattice properties are supplementary geometry, not preference criteria used in the main argument.

Normalization retains the signed product interaction. Let $E_A = \mathcal{E}_{\alpha,\beta}(A)$, $E_B = \mathcal{E}_{\alpha,\beta}(B)$, and write

$$A_\beta = S_A^{1-\beta} - 1, \qquad B_\beta = S_B^{1-\beta} - 1, \qquad C_\beta = (S_A S_B)^{1-\beta} - 1.$$

Then, for $\beta \neq 1$,

$$\mathcal{E}_{\alpha,\beta}(A \times B) = \frac{A_\beta}{C_\beta} E_A + \frac{B_\beta}{C_\beta} E_B + \frac{A_\beta B_\beta}{C_\beta} E_A E_B. \tag{23}$$

The bilinear coefficient is positive for $\beta < 1$ and negative for $\beta > 1$. At $\beta = 1$,

$$\mathcal{E}_{\alpha,1}(A \times B) = \frac{\log S_A \, E_A + \log S_B \, E_B}{\log S_A + \log S_B}. \tag{24}$$

These are properties of the chosen aggregation geometry. They do not show that an observed ecological system is empirically synergistic or redundant; such an interpretation would require a model of dependence and an explicit benchmark.

5.3 Richness scaling and asymptotic severity

Consider a sequence of assemblages satisfying

$$D_\alpha(S) \sim c S^\gamma, \qquad c > 0, \quad 0 \leq \gamma \leq 1. \tag{25}$$

The constants are understood to be compatible with $1 \leq D_\alpha(S) \leq S$. The exponent γ records the growth rate of effective diversity relative to richness.

Theorem 13 (Three asymptotic regimes)**.** *Under Eq.* (25)*, as* $S \to \infty$*:*

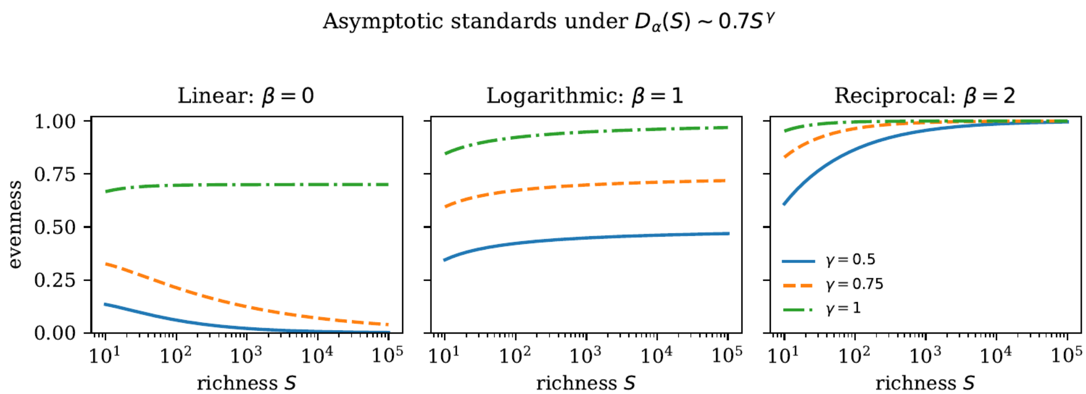

Figure 4: Asymptotic standards under $D_\alpha(S) \sim 0.7S^\gamma$. For sublinear positive growth, the linear geometry tends to zero, the logarithmic geometry tends to γ, and the reciprocal geometry tends to one.

1. *If $\beta < 1$ and $0 < \gamma < 1$,*
$$\mathcal{E}_{\alpha,\beta} \sim c^{1-\beta} S^{-(1-\gamma)(1-\beta)} \to 0.$$
If $\gamma = 1$, then $\mathcal{E}_{\alpha,\beta} \to c^{1-\beta}$. If $\gamma = 0$ and $D_\alpha(S) \to c < \infty$, then $\mathcal{E}_{\alpha,\beta} \to 0$.

2. *If $\beta = 1$, then $\mathcal{E}_{\alpha,1} \to \gamma$.*

3. *If $\beta > 1$ and $\gamma > 0$, then $\mathcal{E}_{\alpha,\beta} \to 1$. If instead $\gamma = 0$ and $D_\alpha(S) \to c < \infty$, then $\mathcal{E}_{\alpha,\beta} \to 1 - c^{1-\beta}$.*

Proof. Substitute Eq. (25) into Eqs. (6)–(7). For $\beta < 1$ and $\gamma > 0$, both power terms diverge and the leading powers yield the stated expression. When $\gamma = 0$, the numerator stays bounded while the denominator diverges. At $\beta = 1$, $\log D_\alpha = \log c + \gamma \log S + o(1)$. For $\beta > 1$, $S^{1-\beta} \to 0$; if $D_\alpha \to \infty$, also $D_\alpha^{1-\beta} \to 0$, whereas bounded D_α gives the stated finite limit. □

The three regions impose different standards. For $\beta < 1$, positive asymptotic evenness requires effective diversity to grow linearly with richness: a proportional-occupation standard. At $\beta = 1$, normalized evenness records the scaling exponent itself. For $\beta > 1$, any unbounded effective-diversity growth eventually appears maximally even: an absolute-growth standard.

A stylized i.i.d.-abundance specialization, useful for linking these regimes to moments of raw abundance distributions, is provided in Appendix C.

5.4 Replication response

Consider K disjoint replicas of an assemblage, with unique category labels in each replica. Hill replication gives $D_\alpha^{(K)} = KD_\alpha$ and $S^{(K)} = KS$. The value-constrained surface is replication-monotone rather than replication-invariant, but the asymptotic response has three distinct regimes.

Theorem 14 (Replication-response trichotomy)**.** *Let $1 < D_\alpha < S$ and $K \to \infty$. Then*

1. *If $\beta < 1$,*
$$\mathcal{E}_{\alpha,\beta}^{(K)} \to \left(\frac{D_\alpha}{S}\right)^{1-\beta}, \tag{26}$$
so the evenness deficit tends to the positive constant $1 - (D_\alpha/S)^{1-\beta}$, with an $O(K^{-(1-\beta)})$ correction.

2. *If $\beta = 1$,*
$$1 - \mathcal{E}_{\alpha,1}^{(K)} = \frac{\log(S/D_\alpha)}{\log(KS)} \sim \frac{\log(S/D_\alpha)}{\log K}. \tag{27}$$

3. If $\beta > 1$,

$$1 - \mathcal{E}_{\alpha,\beta}^{(K)} \sim \left(D_\alpha^{1-\beta} - S^{1-\beta} \right) K^{-(\beta-1)}. \tag{28}$$

A derivation is given in Appendix D.

For non-uniform assemblages, none of the value-constrained sections is replication-invariant at finite K. The section $\beta = 0$ is nevertheless distinctive: Eq. (26) becomes

$$\mathcal{E}_{\alpha,0}^{(K)} \longrightarrow \frac{D_\alpha}{S},$$

exactly the Hill evenness recommended within the Lorenz-consistent framework. If replication invariance is itself non-negotiable, the natural measure is D_α/S rather than a member of the fixed-range family. Within the present surface, β instead determines the form and severity of the departure from that benchmark.

6 Relative merits of the five canonical families

A merit is conditional on a measurement purpose. The five canonical paths differ in how they represent the same order-specific effective diversity once α has been chosen.

6.1 Fixed-β geometries

E_3**: linear effective-diversity geometry.** $E_3 = (D_\alpha - 1)/(S - 1)$ places effective diversity affinely between its lower and upper bounds. An increment from $D_\alpha = 2$ to 3 has the same numerical size as an increment from 20 to 21. Its advantage is direct interpretability and uniform absolute resolution in effective-diversity units. Its trade-off is asymptotic severity: sublinear growth of D_α forces $E_3 \to 0$. Under repeated replication, however, E_3 does not collapse to one; its limit is the replication-invariant Hill ratio D_α/S.

E_5**: logarithmic geometry.** $E_5 = \log D_\alpha / \log S$ gives equal weight to equal multiplicative changes on the underlying logarithmic scale. Under $D_\alpha \sim cS^\gamma$, $E_5 \to \gamma$, and under independent products it aggregates as a log-richness-weighted mean. Its trade-off is that it does not measure the affine position of D_α within $[1, S]$; multiplicative constants vanish asymptotically. Under replication it approaches one, but only logarithmically.

E_4**: reciprocal geometry.** $E_4 = (1-D_\alpha^{-1})/(1-S^{-1})$ has slope proportional to D_α^{-2} and therefore devotes high resolution to the concentrated region. It is useful when the distinction between one and a few effective categories matters more than distinctions among already diverse assemblages. The same concavity produces rapid saturation: if D_α diverges as richness increases, $E_4 \to 1$ even when $D_\alpha/S \to 0$; under replication its deficit decays at rate K^{-1}.

For the same D_α, $E_4 > E_5 > E_3$. This is not disagreement about which assemblage is more even; it is disagreement about numerical severity. Equation (20) supplies the exact largest possible magnitude of that disagreement at a given S.

6.2 Coupled geometries

The paths E_1 and E_2 change β together with α. For any smooth coupling $\beta = f(\alpha)$,

$$\frac{\mathrm{d}}{\mathrm{d}\alpha}\mathcal{E}_{\alpha,f(\alpha)} = \frac{\partial \mathcal{E}}{\partial D_\alpha}\frac{\mathrm{d}D_\alpha}{\mathrm{d}\alpha} + \frac{\partial \mathcal{E}}{\partial \beta} f'(\alpha). \tag{29}$$

For non-uniform distributions, $\mathrm{d}D_\alpha/\mathrm{d}\alpha \leq 0$, while monotonicity in β gives $\partial\mathcal{E}/\partial\beta > 0$. Along E_1, $f'(\alpha) = 1$: increasing order lowers D_α but simultaneously raises β, so the cardinal channel offsets part of the order-induced decline relative to a fixed-β counterfactual. Along E_2, $f'(\alpha) = -1$, so the two

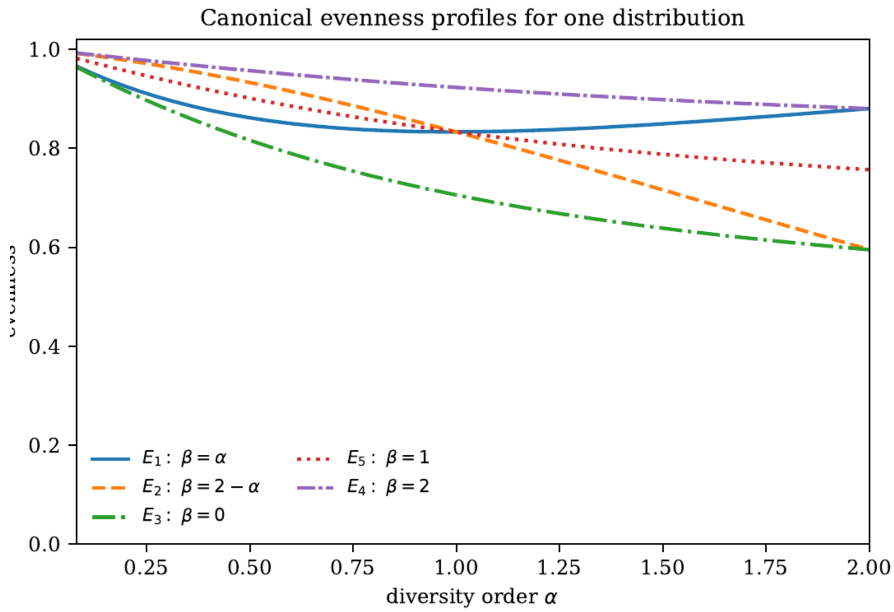

Figure 5: Canonical profiles for $p = (0.40, 0.30, 0.20, 0.07, 0.03)$. The fixed-$\beta$ families differ in numerical geometry at each order; E_1 and E_2 additionally couple the geometry to α.

channels reinforce the decline. In particular, whenever D_α is strictly decreasing in α, E_2 is strictly decreasing as well.

This decomposition should not be mistaken for additional distributional information. It describes how a path through the two-parameter surface combines an order change with a simultaneous change of numerical geometry.

For practical comparison, Table 1 summarizes these trade-offs. It is a decision map, not a ranking. The maximum-spread theorem also prevents qualitative language such as "more permissive" from floating free of scale: the total numerical effect available to the choice of fixed geometry is bounded by richness.

7 Numerical and ecological illustration

7.1 The common surface

For $p = (0.40, 0.30, 0.20, 0.07, 0.03)$, Figure 6 shows the normalized surface over $0.05 \le \alpha \le 2$ and $0 \le \beta \le 2$. At fixed α, moving in β changes only the numerical representation of the same D_α; moving in α changes the order-sensitive effective diversity itself.

7.2 A worked empirical crosswalk

We use the public Alpine succession data analyzed by Chao and Ricotta (2019) for a worked crosswalk; no new ecological inference is intended. Fix $\alpha = 2$. In the early-succession assemblage, $S = 35$ and $D_2 = 18.28$. At this order $E_2 = E_3$ because both have $\beta = 0$, while $E_1 = E_4$ because both have $\beta = 2$.

If the logarithmic family reports $E_5 = 0.8173$, Eq. (17) gives

$$D_2 = S^{E_5} = 35^{0.8173} \approx 18.28.$$

Table 1: Relative merits as consequences of the Sharma–Mittal representation.

Family	Geometry	Interpretive use	Main trade-off
E_3	$\beta = 0$, linear in D_α	Linear position in the effective-diversity interval; equal absolute resolution; exact replication limit D_α/S.	Severe under sublinear richness growth; can report low evenness despite many effective categories in absolute terms.
E_5	$\beta = 1$, logarithmic	Natural scaling and multiplicative interpretation; $E_5 \to \gamma$ under $D_\alpha \sim S^\gamma$; log-richness-weighted product aggregation.	Does not measure D_α/S or affine occupation; multiplicative constants are asymptotically lost; replication drives it to one logarithmically.
E_4	$\beta = 2$, reciprocal	High resolution near maximal concentration; useful for distinguishing monopoly or strong dominance from modest diversification.	Rapid saturation under richness growth and replication; tends to one whenever D_α diverges.
E_1	$\beta = \alpha$	Couples order and geometry so that the cardinal channel locally offsets part of the order-induced decline.	Can attenuate contrasts that an order profile is intended to expose.
E_2	$\beta = 2 - \alpha$	Couples order and geometry so that both channels reinforce order-induced decline; useful when contrast across orders is the target.	Cardinal values become more order-dependent and can accentuate profile movement.

The same D_2 gives

$$E_3 = \frac{D_2 - 1}{S - 1} \approx 0.5082, \qquad E_4 = \frac{1 - D_2^{-1}}{1 - S^{-1}} \approx 0.9731.$$

These are exact crosswalks, up to rounding, of the same order-specific effective diversity under three geometries.

The maximum-spread theorem makes the magnitude interpretable. At $S = 35$, the largest possible difference between any two sections in $0 \le \beta \le 2$ is

$$\frac{\sqrt{35} - 1}{\sqrt{35} + 1} \approx 0.7108.$$

The observed early-stage spread is $0.9731 - 0.5082 = 0.4649$, which is 65.4% of that theoretical maximum. The corresponding proportions are 64.5% for the mid-succession stage and 60.1% for the late stage. The empirical differences are therefore not merely large in raw units; they occupy a substantial, quantifiable fraction of the cardinal freedom available at the respective richness values.

At common S and α, two represented population formulas cannot reverse an assemblage ranking. A ranking reversal in published results must therefore come from another source: a different Hill order, different richness, a different estimator or sampling realization, or a measure not mediated by the same D_α. The next example takes the second possibility directly.

7.3 A coverage-standardized rank reversal

Chao et al. (2020) compare Miocene and Pliocene ostracod assemblages at a common maximum standardized coverage $C_{\max} = 99.3\%$. Their Step 3 reports standardized richness $S(C_{\max})$ and Shannon diversity $D_1(C_{\max})$ of $(30.2, 11.0)$ for the Miocene and $(185.5, 25.6)$ for the Pliocene. Their Step 4 reports the corresponding $\beta = 0$ class and Pielou's $\beta = 1$ index, both of which rank the Miocene as more even. Applying the reciprocal class $E_4 = \mathcal{E}_{1,2}$ to those same standardized values reverses the ordering.

The sufficient criterion in Proposition 7 is satisfied: the linear section ranks Miocene > Pliocene,

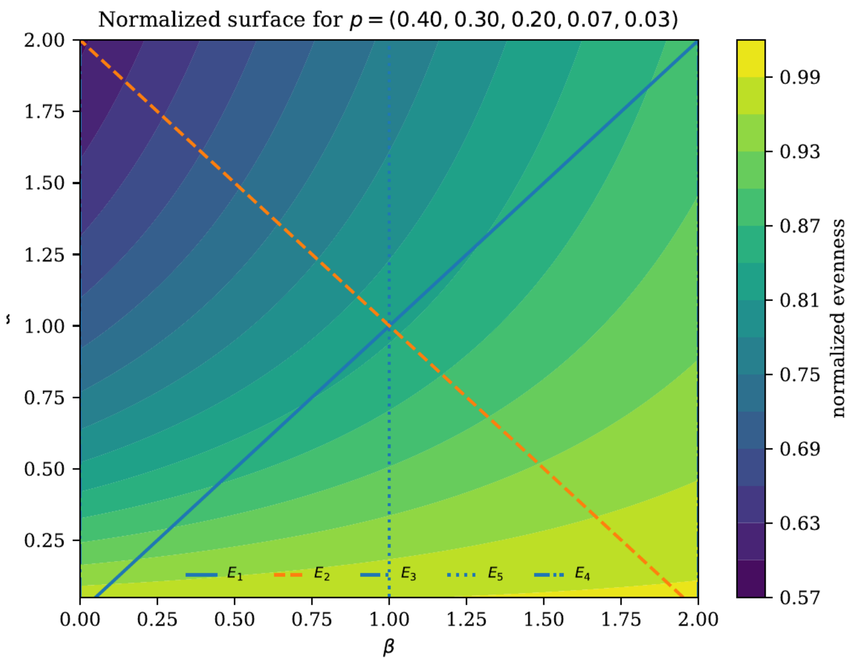

Figure 6: Normalized evenness surface for $p = (0.40, 0.30, 0.20, 0.07, 0.03)$. The diagonal and anti-diagonal are E_1 and E_2; the vertical sections are E_3, E_5, and E_4 at $\beta = 0, 1, 2$.

Table 2: Three canonical cardinalizations of the coverage-standardized values reported by Chao et al. (2020). Values are calculated from their published Table 2, which is rounded to one decimal place for S and D_1.

Assemblage	$S(C_{\max})$	$D_1(C_{\max})$	$\mathcal{E}_{1,0}$	$\mathcal{E}_{1,1}$	$\mathcal{E}_{1,2}$
Miocene	30.2	11.0	0.3425	0.7036	0.9402
Pliocene	185.5	25.6	0.1333	0.6208	0.9661

whereas effective diversity itself ranks Pliocene > Miocene. Solving

$$\mathcal{E}_{1,\beta}(11.0; 30.2) = \mathcal{E}_{1,\beta}(25.6; 185.5)$$

with the published rounded values gives

$$\beta^* \approx 1.40.$$

The result is not sensitive to the one-decimal rounding in the source table. Allowing each published S and D_1 value to vary independently by ± 0.05 gives $\beta^* \in [1.3865, 1.4067]$; over the same box, $\mathcal{E}_{1,2}(\text{Miocene}) - \mathcal{E}_{1,2}(\text{Pliocene})$ remains between -0.0265 and -0.0254. The first two evenness columns in Table 2 reproduce the values reported by Chao et al. at their published precision: 0.34/0.13 for the $\beta = 0$ class and 0.70/0.62 for Pielou. Only the $\mathcal{E}_{1,2}$ column is added here. Their separate Step-4 column labelled $q = 2$ is a different quantity, $\mathcal{E}_{2,0}$: it changes the Hill order while retaining $\beta = 0$, whereas the present reversal holds $\alpha = 1$ fixed and changes β.

This is not a correction to Chao et al. (2020). Their statement that all measures they report rank the Miocene as more even is correct; the reversal appears along the cardinal axis introduced here, and $\beta = 2$ is itself the canonical E_4 class of Chao and Ricotta (2019).

The example also shows the cost of the reversal. At $\beta = 2$ both values are close to one and differ by only about 0.026. The rank transition therefore occurs in a region of strong cardinal compression. That is the same geometry seen from the other side: increasing β shifts the cross-richness ordering toward D_α while simultaneously reducing numerical resolution among already diverse assemblages.

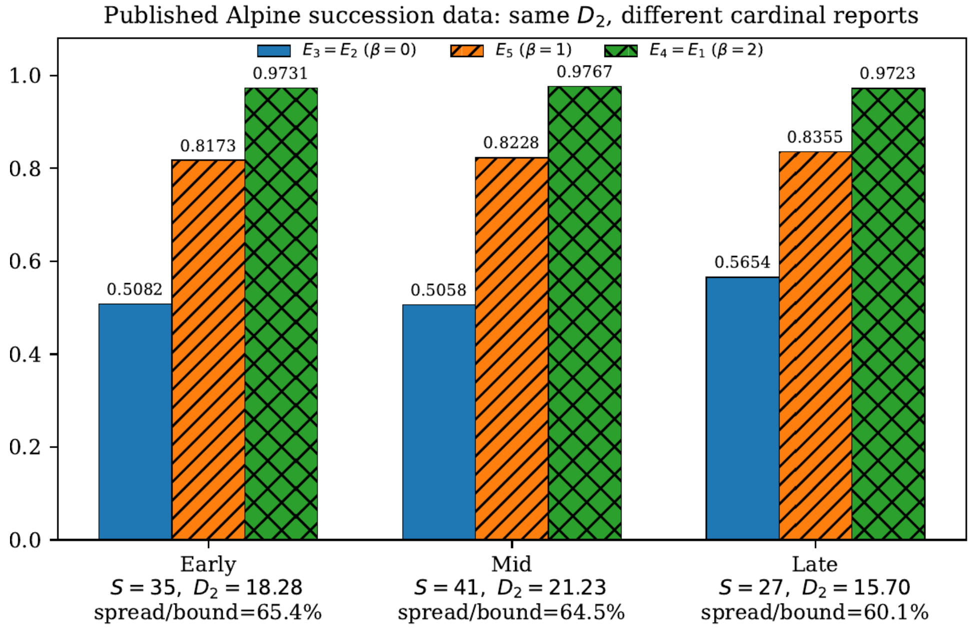

Figure 7: Cardinal reports for the Alpine succession data at $\alpha = 2$. Richness, D_2, and the observed $E_4 - E_3$ spread as a proportion of the theoretical maximum in Eq. (20) are shown for each stage. Relative-abundance data are from the public materials accompanying Chao and Ricotta (2019).

8 Discussion

8.1 What the cardinal parameter changes

Once richness and Hill order are fixed, every represented class is a one-to-one transformation of the same D_α. The selection problem is therefore not about identifying a uniquely correct scalar summary of the abundance distribution. It concerns the numerical meaning assigned to an already selected order-specific effective diversity.

The local and global results are complementary. The endpoint ratio S^β states where a scale spends its local resolution. The maximum-spread bound states how much the entire choice of $\beta \in [0, 2]$ can change a normalized report. A large local skew does not automatically imply an arbitrarily large total discrepancy; the latter is exactly bounded by $(\sqrt{S} - 1)/(\sqrt{S} + 1)$. Across different richness levels, a further effect becomes possible: the same change in cardinal geometry can alter the ranking itself. Proposition 7 gives a sufficient condition, and the coverage-standardized Miocene–Pliocene comparison supplies a published example.

8.2 Invariant and non-invariant conclusions

At fixed S and α, rankings, equality, endpoints, and any statement depending only on monotone order are invariant in β. Cardinal quantities are not. Absolute differences, ratios, arithmetic averages, thresholds, and regression coefficients expressed on the raw evenness scale can change substantially.

For example, with $S = 100$, compare $D_\alpha = 10$ and $D_\alpha = 20$. Their ordering is unchanged, but the absolute gap is approximately 0.1010 for $\beta = 0$, 0.1505 for $\beta = 1$, and 0.0505 for $\beta = 2$. This does not indicate disagreement about the underlying effective-diversity order; it reflects a different assignment of numerical distance. The fixed-richness qualification is essential: Section 7.3 shows that when S changes, a ranking reversal can occur even at a common α.

The distinction matters for comparative work. If S, α, and the formula are known, Eq. (17)

provides an exact crosswalk through D_α. Conversely, pooling raw evenness values produced by different geometries is generally unjustified merely because all are normalized to $[0, 1]$.

8.3 Relative merits without a universal winner

The fixed-β families correspond to different measurement purposes. E_3 is natural for affine occupation of an effective-diversity capacity; E_5 for multiplicative scaling and growth exponents; E_4 for fine discrimination near strong concentration. Across unequal richness, higher-β sections can also alter a ranking when richness-normalized occupation and effective diversity order the assemblages differently. The coupled paths address a different issue: E_1 offsets part of the numerical movement induced by increasing order, whereas E_2 reinforces it. None is universally preferable.

The new replication result makes the asymmetry among these choices more explicit without changing that conclusion. If replication invariance is a governing axiom, no value-constrained section is the right object. If fixed endpoints across richness are instead retained, low-β sections preserve more of the Hill-ratio benchmark under replication, while high-β sections devote more cardinal resolution to strong concentration and saturate more rapidly elsewhere. Across unequal richness, movement toward higher β can also cross a rank threshold when richness-normalized occupation and D_α order the assemblages differently, as in Section 7.3.

This conditional conclusion is compatible with both sides of the current ecological debate: recent critiques warn against treating evenness as a self-interpreting ecological state variable (Alroy, 2025; Warren, 2026), whereas other recent work documents ecosystem-function relationships that are robust across several evenness measures (Hordijk, 2026). The present framework does not decide that empirical debate. It instead makes the numerical judgment embedded in a chosen formula explicit, which is a prerequisite for deciding whether that judgment is useful in a given application.

8.4 Replication invariance and value constraints

Chisholm (2026) returns to the Lorenz-consistency tradition and recommends replication-invariant measures, including Hill evenness D_α/S. The same paper emphasizes that the value-constraint requirement—in particular, a richness-independent minimum—is incompatible with the full Lorenz-consistency axioms, following the earlier argument of Gosselin (2001). If replication invariance is dropped, Pielou's index and Heip's index satisfy the resulting alternative axiomatization; these are exactly the $\alpha = 1$, $\beta = 1$ and $\beta = 0$ points of the present surface.

Theorem 14 does not reconcile the two axiomatic programs. It quantifies their separation. For $\beta < 1$, replication leaves a positive evenness deficit; at $\beta = 0$ the limiting value is exactly the Hill ratio. At $\beta = 1$ the deficit vanishes only as $1/\log K$, while for $\beta > 1$ it vanishes polynomially. Thus β controls not merely whether replication invariance is violated, but the asymptotic form of that violation.

8.5 How much should be inferred from product interaction?

The sign of $1 - \beta$ has a precise compositional meaning under independent products: it determines whether Eq. (22) contains a positive, zero, or negative interaction term. It is not evidence that observed ecological categories are synergistic or redundant. β is selected by the analyst; it is not estimated from a single abundance vector. Empirical claims about dependence, overlap, or complementarity require observed subsystems and an explicit independence or conditional benchmark.

8.6 Position relative to earlier parametric and Sharma–Mittal work

Three antecedents delimit the claim. First, Hill's double-continuum evenness and later parametric evenness work vary diversity orders and compare effective numbers (Hill, 1973; Ricotta and Avena, 2002; Ricotta, 2003). Second, Hoffmann and Crupi place diversity measures in a Sharma–Mittal order–degree plane (Hoffmann, 2008; Crupi, 2019); a recent mathematical-biology review likewise treats Sharma–Mittal as an established generalized-entropy family (Mondaini and de Albuquerque Neto, 2024). Third, fixed-order generalized entropies that are monotone functions of the same power sum have the same number equivalent (Jost, 2009). Accordingly, neither the Sharma–Mittal plane, maximum normalization as a generic device, nor fixed-order ordinal equivalence is claimed here as new.

The contribution claimed here is narrower and testable. The maximum-normalized Sharma–Mittal surface used here contains the five Hill-based classes of Chao and Ricotta (2019) as exact restrictions; the whole finite-β surface satisfies their Requirements 1a–3b; and the surface yields quantitative consequences for comparison among those classes. These include the endpoint resolution ratio S^β, the sharp global spread bound in Eq. (20), the sufficient cross-richness reversal criterion, the normalized independent-product law, the richness-scaling regimes, and the replication-response trichotomy. To our knowledge, this package has not previously been formulated as a two-parameter geometry of evenness.

8.7 Relation to distance-based evenness frameworks

The construction does not subsume every admissible or proposed evenness measure. Chao and Ricotta also report the Minkowski-distance family discussed by Kvålseth (2015). In general, a Minkowski distance from uniformity is not determined by a single Hill number and can retain distributional information that one D_α compresses away.

The Euclidean member is an instructive boundary case. Writing the normalized Minkowski evenness of order two as M_2, one obtains

$$M_2 = 1 - \sqrt{\frac{D_2^{-1} - S^{-1}}{1 - S^{-1}}} = 1 - \sqrt{\frac{S - D_2}{D_2(S-1)}}. \tag{30}$$

Thus M_2 is Hill-sufficient at order two, but it is not a finite-β section of Eq. (6). As $D_2 \uparrow S$, its derivative diverges like $(S - D_2)^{-1/2}$, whereas every finite Sharma–Mittal section at order two has finite slope at uniformity. Hence, at order two, Hill-sufficiency alone does not imply membership in the finite-β Sharma–Mittal family. Appendix E gives the short derivation.

Chisholm's (2026) mean pairwise similarity, $1 - G$, marks a different boundary. With

$$1 - G = 1 - \frac{1}{S}\sum_{i<j} |p_i - p_j|,$$

it need not be determined by the Hill number at a fixed order. For example, the two four-species distributions $(0.45, 0.30, 0.20, 0.05)$ and $(0.50, 0.20, 0.15, 0.15)$ have the same Simpson concentration, $\sum_i p_i^2 = 0.335$, and hence exactly the same $D_2 = 200/67 \approx 2.9851$, whereas $1 - G$ equals 0.675 and 0.725, respectively. Thus, at order two, $1 - G$ is not even a function of D_2. This is distinct from M_2: the latter is Hill-sufficient at order two but lies outside the finite-β Sharma–Mittal family because of its endpoint-slope singularity.

8.8 Limitations and next steps

Sampling theory remains outside the main argument. Smooth monotone re-expression rescales both a local signal and its standard error by the same first derivative at first order, so Eq. (8) does not by itself imply a generic precision advantage for any β. Curvature-induced bias, unseen species, and uncertainty in realized richness are second-order or upstream inferential issues and require a separate sampling analysis. The coverage-standardized Chao et al. example is used here only to hold sample completeness common while illustrating the cardinal geometry; it does not supply a sampling theory for the surface.

The paper also focuses on the canonical square $0 \leq \beta \leq 2$. The full finite-β family is admissible under the stated requirements, but mathematical availability does not by itself justify additional paths $\beta = f(\alpha)$. New restrictions should be tied to an independently motivated symmetry, composition rule, decision criterion, or empirical target.

Finally, the representation theorem is not an axiomatic necessity theorem. A stronger result would identify assumptions under which maximum-normalized Sharma–Mittal evenness is the required form of a Hill-sufficient measure with specified composition or resolution properties. The sufficient reversal criterion likewise does not assert uniqueness of the crossing; a general single-crossing characterization remains open.

9 Conclusion

Maximum normalization of Sharma–Mittal entropy produces a two-parameter family of admissible evenness measures. Five important Hill-based classes are exact paths on this surface. At fixed richness and order, all represented sections are ordinally equivalent, so the choice among them changes numerical spacing rather than the order-specific scalar information being ranked. Across different richness levels, that fixed-S protection can fail, and the same cardinal parameter can change the ranking itself.

The parameter β has several precise interpretations. It reallocates local resolution, with endpoint skew S^{β}, and it bounds global disagreement on the canonical square through $(\sqrt{S}-1)/(\sqrt{S}+1)$. Across unequal richness, it can also move a comparison from richness-normalized occupation toward an ordering increasingly dominated by D_α.

The same parameter determines the sign of the interaction term under independent-product composition, imposes a distinct asymptotic standard on effective-diversity growth relative to richness, and controls the asymptotic response to replication. The last result sharpens the relation to the Lorenz-consistency debate: $\beta = 0$ converges under replication to Hill evenness D_α/S, whereas $\beta \geq 1$ ultimately collapses toward one.

No value of β is selected by the abundance vector alone. An evenness index should therefore be chosen by stating the numerical question it is intended to answer. The Sharma–Mittal surface makes those choices visible and mathematically comparable without claiming that one geometry is universally correct.

A Proof of monotonicity in β

Fix $1 < D_\alpha < S$ and define

$$r = \frac{\log D_\alpha}{\log S} \in (0,1), \qquad t = S^{1-\beta} > 0.$$

Then $D_\alpha^{1-\beta} = t^r$, so

$$\mathcal{E}_{\alpha,\beta} = \psi_r(t) = \frac{t^r - 1}{t - 1},$$

with continuous value $\psi_r(1) = r$. For $0 < r < 1$, t^r is strictly concave. The chord slope from the fixed point $(1,1)$ to (t, t^r) is therefore strictly decreasing in t. Since $t = S^{1-\beta}$ is strictly decreasing in β, $\mathcal{E}_{\alpha,\beta}$ is strictly increasing in β.

B Majorization-lattice qualification

Bruno and Vaccaro (2026) establish lattice subadditivity for $\alpha \geq 0$, $\beta \geq 1$ and supermodularity for $\alpha > 0$, $\beta \leq \alpha$ for unnormalized Sharma–Mittal entropy. Under the realized-richness convention, transferring these inequalities to normalized evenness requires a common support size.

Restrict attention to the interior $\mathcal{P}_S^\circ = \{p \in \mathcal{P}_S : p_i > 0 \,\forall i\}$, with vectors arranged in non-increasing order. Let $P_k = \sum_{i \leq k} p_i$ and $Q_k = \sum_{i \leq k} q_i$. For the meet,

$$(p \wedge q)_k = \min(P_k, Q_k) - \min(P_{k-1}, Q_{k-1}) \geq \min(p_k, q_k) > 0.$$

For the raw cumulative-maximum construction of the join, the analogous inequality with max gives strictly positive increments; the standard flattening step averages positive coordinates and therefore preserves strict positivity. Hence $p, q, p \wedge q$, and $p \vee q$ all retain realized richness S. Dividing by the common positive maximum $\mathrm{SM}^{\max}_{\alpha,\beta}(S)$ preserves the relevant lattice inequalities. On boundary vectors containing zeros, the unnormalized lattice statements remain valid on a fixed ambient dimension, but a common realized-richness normalization need not survive.

Within the canonical square this yields the following sufficient-property placement. E_3 ($\beta = 0$) is supermodular for every $\alpha > 0$. E_1 ($\beta = \alpha$) is supermodular along its path and is also lattice-subadditive for $\alpha \geq 1$. E_5 ($\beta = 1$) is lattice-subadditive for every $\alpha > 0$ and supermodular for $\alpha \geq 1$. E_4 ($\beta = 2$) is lattice-subadditive throughout the square and reaches the guaranteed supermodular region at $\alpha = 2$. Finally, E_2 ($\beta = 2 - \alpha$) lies in the guaranteed lattice-subadditive region for $0 < \alpha \leq 1$ and the guaranteed supermodular region for $1 \leq \alpha \leq 2$. These are sufficient regions, not converse characterizations.

C An i.i.d. abundance specialization

Let raw abundances $N_1, N_2, \ldots$ be i.i.d. positive random variables, $p_i = N_i/T_S$, $T_S = \sum_{i \leq S} N_i$, and assume the required moments are finite. Write $m = \mathbb{E}[N]$ and $\mu_\alpha = \mathbb{E}[N^\alpha]$. For $\alpha \neq 1$, the strong law gives

$$\frac{D_\alpha}{S} \longrightarrow c_\alpha = \left(\frac{\mu_\alpha}{m^\alpha}\right)^{1/(1-\alpha)} \qquad \text{a.s.} \tag{31}$$

For $\alpha = 1$, assuming $\mathbb{E}[N|\log N|] < \infty$,

$$\frac{D_1}{S} \longrightarrow c_1 = m \exp\left(-\frac{\mathbb{E}[N \log N]}{m}\right) \qquad \text{a.s.} \tag{32}$$

Thus this model is the $\gamma = 1$ case of the scaling theorem. It follows that

$$\mathcal{E}_{\alpha,\beta} \longrightarrow \begin{cases} (\mu_\alpha/m^\alpha)^{(1-\beta)/(1-\alpha)}, & \beta < 1,\ \alpha \neq 1, \\ m^{1-\beta} \exp(-(1-\beta)\mathbb{E}[N \log N]/m)\,, & \beta < 1,\ \alpha = 1, \\ 1, & \beta \geq 1. \end{cases}$$

At $\alpha = 2$, $\beta = 0$, writing $CV^2 = \mathrm{Var}(N)/m^2$ gives $\mu_2/m^2 = 1 + CV^2$, and therefore

$$E_3^2 \longrightarrow \frac{1}{1 + CV^2}.$$

This is a stylized probabilistic specialization, not an assumption required by the main results.

D Replication monotonicity and asymptotic response

Consider K disjoint replicas of an assemblage, each with unique category labels. Hill replication gives $D_\alpha^{(K)} = KD_\alpha$ and $S^{(K)} = KS$, hence

$$\mathcal{E}_{\alpha,\beta}^{(K)} = \frac{(KD_\alpha)^{1-\beta} - 1}{(KS)^{1-\beta} - 1}. \tag{33}$$

For a non-uniform original assemblage $D_\alpha < S$, differentiation with respect to continuous $K > 0$ shows that this expression increases with K for every finite β. At $\beta = 1$,

$$\mathcal{E}_{\alpha,1}^{(K)} = \frac{\log K + \log D_\alpha}{\log K + \log S},$$

which is likewise increasing. Thus replication monotonicity extends from the five canonical classes discussed by Chao and Ricotta (2019) to the entire normalized Sharma–Mittal surface.

For the asymptotic regimes, write $t = 1 - \beta$. If $\beta < 1$, $t > 0$, and division of numerator and denominator in Eq. (33) by K^t gives

$$\mathcal{E}_{\alpha,\beta}^{(K)} = \frac{D_\alpha^t - K^{-t}}{S^t - K^{-t}} \longrightarrow \left(\frac{D_\alpha}{S}\right)^t,$$

with an $O(K^{-t})$ correction. If $\beta = 1$,

$$1 - \mathcal{E}_{\alpha,1}^{(K)} = \frac{\log(S/D_\alpha)}{\log(KS)}.$$

Finally, if $\beta > 1$, set $r = \beta - 1 > 0$. Then

$$1 - \mathcal{E}_{\alpha,\beta}^{(K)} = \frac{K^{-r}(D_\alpha^{-r} - S^{-r})}{1 - K^{-r}S^{-r}} \sim K^{-r}(D_\alpha^{-r} - S^{-r}),$$

which is Eq. (28).

E Minkowski boundary case

For distance order $r > 0$, normalized Minkowski evenness can be written

$$M_r(p; S) = 1 - \left[\frac{\sum_{i=1}^S |p_i - S^{-1}|^r}{(1 - S^{-1})^r + (S-1)S^{-r}}\right]^{1/r}.$$

For $r = 2$,

$$\sum_i \left(p_i - \frac{1}{S}\right)^2 = \sum_i p_i^2 - \frac{1}{S} = \frac{1}{D_2} - \frac{1}{S},$$

and the denominator simplifies to $1 - S^{-1}$, giving Eq. (30). As $D_2 \uparrow S$,

$$1 - M_2 \sim \sqrt{\frac{S - D_2}{S(S-1)}},$$

so $\partial M_2/\partial D_2$ diverges. By contrast, every finite Sharma–Mittal section has finite slope at uniformity:

$$\left.\frac{\partial \mathcal{E}_{2,\beta}}{\partial D_2}\right|_{D_2=S} = \frac{(1-\beta)S^{-\beta}}{S^{1-\beta} - 1}, \qquad \left.\frac{\partial \mathcal{E}_{2,1}}{\partial D_2}\right|_{D_2=S} = \frac{1}{S\log S}.$$

Data availability

No new empirical data were generated for this study. The Alpine illustration uses the public relative-abundance data accompanying Chao and Ricotta (2019), archived with the article materials at Zenodo (DOI: 10.5281/zenodo.3341384). The Miocene–Pliocene illustration uses the coverage-standardized values reported in Table 2 of Chao et al. (2020). The numerical examples are fully specified by the equations and cited data reported in the manuscript.

Conflict of interest

The author declares no conflict of interest.

References

[1] Alroy, J. 2025. Does evenness even exist? *Ecology Letters* 28: e70181. doi:10.1111/ele.70181.

[2] Bruno, R. and Vaccaro, U. 2026. The Sharma–Mittal entropy is subadditive and supermodular on the majorization lattice. arXiv:2605.18600v3, 26 May 2026.

[3] Chao, A., Chiu, C.-H. and Jost, L. 2014. Unifying species diversity, phylogenetic diversity, functional diversity, and related similarity/differentiation measures through Hill numbers. *Annual Review of Ecology, Evolution, and Systematics* 45: 297–324.

[4] Chao, A. and Ricotta, C. 2019. Quantifying evenness and linking it to diversity, beta diversity, and similarity. *Ecology* 100: e02852. doi:10.1002/ecy.2852.

[5] Chao, A., Kubota, Y., Zelený, D., Chiu, C.-H., Li, C.-F., Kusumoto, B., Yasuhara, M., Thorn, S., Wei, C.-L., Costello, M. J. and Colwell, R. K. 2020. Quantifying sample completeness and comparing diversities among assemblages. *Ecological Research* 35: 292–314. doi:10.1111/1440-1703.12102.

[6] Chisholm, R. A. 2026. The usefulness of evenness. *Ecology Letters* 29: e70446. doi:10.1111/ele.70446.

[7] Crupi, V. 2019. Measures of biological diversity: overview and unified framework. In: Casetta, E., Marques da Silva, J. and Vecchi, D. (eds), *From Assessing to Conserving Biodiversity*. Springer, pp. 123–136. doi:10.1007/978-3-030-10991-2_6.

[8] Gosselin, F. 2001. Lorenz partial order: the best known logical framework to define evenness indices. *Community Ecology* 2: 197–207.

[9] Heip, C. 1974. A new index measuring evenness. *Journal of the Marine Biological Association of the United Kingdom* 54: 555–557.

[10] Hill, M. O. 1973. Diversity and evenness: a unifying notation and its consequences. *Ecology* 54: 427–432.

[11] Hoffmann, S. 2008. Generalized distribution-based diversity measurement: survey and unification. FEMM Working Paper 08023, Otto-von-Guericke University Magdeburg. doi:10.24352/UB.OVGU-2018-364.

[12] Hordijk, I. 2026. Even evenness is important: the direct and mediating effects of species abundances for ecosystem services. *New Phytologist* 250: 1987–1989. doi:10.1111/nph.71101.

[13] Jost, L. 2009. Mismeasuring biological diversity: response to Hoffmann and Hoffmann (2008). *Ecological Economics* 68: 925–928. doi:10.1016/j.ecolecon.2008.10.015.

[14] Jost, L. 2010. The relation between evenness and diversity. *Diversity* 2: 207–232.

[15] Kvålseth, T. O. 1991. Note on biological diversity, evenness, and homogeneity. *Oikos* 62: 123–127.

[16] Kvålseth, T. O. 2015. Evenness indices once again: critical analysis of properties. *SpringerPlus* 4: 232.

[17] Kvålseth, T. O. 2024. Diversity analysis: richness versus evenness. *Ecology and Evolution* 14: e70275. doi:10.1002/ece3.70275.

[18] Marshall, A. W., Olkin, I. and Arnold, B. C. 2011. *Inequalities: Theory of Majorization and Its Applications*, 2nd ed. Springer.

[19] Mendes, R. S., Evangelista, L. R., Thomaz, S. M., Agostinho, A. A. and Gomes, L. C. 2008. A unified index to measure ecological diversity and species rarity. *Ecography* 31: 450–456.

[20] Mondaini, R. P. and de Albuquerque Neto, S. C. 2024. A comprehensive review of Sharma–Mittal entropy measures and their usefulness in the study of discrete probability distributions in mathematical biology. In: Mondaini, R. P. (ed.), *Trends in Biomathematics: Exploring Epidemics, Eco-Epidemiological Systems, and Optimal Control Strategies*. Springer, pp. 321–355. doi:10.1007/978-3-031-59072-6_16.

[21] Pielou, E. C. 1966. The measurement of diversity in different types of biological collections. *Journal of Theoretical Biology* 13: 131–144.

[22] Rényi, A. 1961. On measures of entropy and information. In: *Proceedings of the Fourth Berkeley Symposium on Mathematical Statistics and Probability*, Vol. 1, pp. 547–561. University of California Press.

[23] Ricotta, C. and Avena, G. C. 2002. On the information-theoretical meaning of Hill's parametric evenness. *Acta Biotheoretica* 50: 63–71. doi:10.1023/A:1014717428386.

[24] Ricotta, C. 2003. On parametric evenness measures. *Journal of Theoretical Biology* 222: 189–197.

[25] Routledge, R. D. 1983. Evenness indices: are any admissible? *Oikos* 40: 149–151.

[26] Shannon, C. E. 1948. A mathematical theory of communication. *Bell System Technical Journal* 27: 379–423, 623–656.

[27] Sharma, B. D. and Mittal, D. P. 1975. New non-additive measures of entropy for discrete probability distributions. *Journal of Mathematical Sciences (Delhi)* 10: 28–40.

[28] Smith, B. and Wilson, J. B. 1996. A consumer's guide to evenness indices. *Oikos* 76: 70–82.

[29] Tsallis, C. 1988. Possible generalization of Boltzmann–Gibbs statistics. *Journal of Statistical Physics* 52: 479–487.

[30] Tuomisto, H. 2012. An updated consumer's guide to evenness and related indices. *Oikos* 121: 1203–1218.

[31] Warren, R., II. 2026. The evenness illusion. *Basic and Applied Ecology* 94: 44–48. doi:10.1016/j.baae.2026.05.003.